 CMC, vol.17, no.2, pp.103-125, 2010

A Novel Framework for Building Materials Knowledge Systems

Surya R. Kalidindi[1,2,3], Stephen R. Niezgoda[1], Giacomo Landi[1] Shraddha Vachhani[1] and Tony Fast[1]

Abstract: This paper presents a novel mathematical framework for building a comprehensive materials knowledge system (MKS) to extract, store and recall hierarchical structure-property-processing linkages for a broad range of material systems. This new framework relies heavily on the use of computationally efficient FFT (Fast Fourier Transforms)-based algorithms for data-mining local structure-response-structure evolution linkages from large numerical datasets produced by established modelling strategies for microscale phenomena. Another salient feature of this new framework is that it facilitates flow of high fidelity information in both directions between the constituent length scales, and thereby offers a new strategy for concurrent multi-scale modelling of materials phenomena. The viability of this new approach is demonstrated in this paper with two selected case studies: (i) rigid-plastic deformation of a two-phase composite material, and (ii) spinodal decomposition of a binary alloy.

1 Introduction

The core activity in the field of Materials Science and Engineering is the establishment of robust microstructure-property-processing relationships for a broad range of materials systems. These relationships are central to the design and development of new materials with enhanced properties or performance characteristics. However, the pace at which such relationships are being established currently by the experts in this field is exceedingly slow. For example, it is often reported that it takes about twenty years [Schafrik (2003)] to design, process, and insert a new material in an advanced technology application. This is largely attributed to the fact that the current process of new materials development relies heavily on experimental discovery, which is often slow and very expensive. Furthermore, the

[1] Department of Materials Science and Engineering, Drexel University, Philadelphia, 19104
[2] Department of Mechanical Engineering and Mechanics, Drexel University, Philadelphia 19104
[3] Author to whom correspondence should be addressed

practitioners in this relatively young field have not yet adopted a mathematically rigorous framework for the description of the microstructure (i.e. internal structure) of the material. The internal structure of most material systems spans a multitude of length scales, from the atomistic to the macroscale. However, the general practice for microstructure quantification is to define and extract physically meaningful, statistically based (stereological), metrics to capture the salient features of the microstructure, and use them to formulate structure-property relationships of interest. In reality, these metrics tend to be highly simplified and include parameters such as average crystal size and texture [Bunge (1993)] for single-phase polycrystalline materials, and phase volume fractions and their average shape and spacing for multi-phase composites. These grossly simplified intuitive measures of microstructure are typically inadequate for establishing reliable structure-property-processing relationships.

In the opinion of the authors, another major deficiency of the approach used currently by materials scientists and engineers is the fact that their efforts are focused largely on establishing the correlations between macroscale (effective) properties and the ensemble averaged statistical measures of the microstructure. As such, these correlations do not provide any insight into how the imposed load at the macroscale is distributed at the microscale (also called localization). In other words, the information flow in these correlations is primarily from the microscale to the macroscale, with no feedback in the opposite direction. As an example, let us consider the well-known Hall-Petch relation [Hall (1951); Petch (1953)] that correlates the macroscale yield strength in a polycrystalline sample to the average grain size associated with the microstructure. Although this correlation helps us establish the macroscale property of interest based on a simple microstructure parameter, it says nothing about how the imposed stress (or strain) is distributed among the constituent grains of different sizes. The information on how the imposed stress (or strain) is localized at the microscale is expected to play a key role in many of the defect-sensitive properties of interest in the material (e.g. the fatigue strength).

The authors assert that several recent advances in microstructure quantification and multi-scale modeling have now set the stage for a new, transformative, approach to establishing the essential knowledge systems that lie at the core of the activities in the Materials Science and Engineering. It is now possible to capture the rich three-dimensional details of the material structure at various length scales (e.g. X-ray micro-tomography [Flannery et al. (1987); Maire et al. (2001)] automated serial sectioning [Alkemper and Voorhees (2001); Sivel et al. (2004)], 3-D atom probe [Blavette et al. (1993); Seidman (2007)]). Methods for rigorous quantification of the microstructure statistics are gaining wider acceptance in the materials

community [Adams and Olson (1998); Torquato (2002); Adams et al. (2005); Mason and Adams (1999); Fullwood et al. (2009); Saheli et al. (2004); Beran et al. (1996); Zeman and Ejnoha (2007); Sankaran and Zabaras (2006); Tewari et al. (2004); Gusev et al. (2000)]. Major strides are being made in the development of multi-scale materials modelling strategies spanning atomistic simulations [Li et al. (2002); Yamakov et al. (2004)], dislocation dynamics [Zbib et al. (1998); Amodeo and Ghoniem (1990)], finite element models [Zienkiewicz and Taylor (2005)] and phase-field models [Wheeler et al. (1992); Li et al. (2005); Kazaryan et al. (2000); Shen and Wang (2003)]. It is now possible to incorporate very complex physics in numerical models to accurately simulate local behavior at any selected length scale, including details of the inherent anisotropy. In order to exploit these recent advances, it behooves us to establish computationally efficient *materials knowledge systems* (MKS), where information flows in both directions with minimal loss between any selected hierarchical length scales of interest. A major goal of MKS is to facilitate computationally efficient concurrent multi-scale materials modelling strategies that are also aimed at solving inverse problems of materials design (i.e. optimizing material microstructure to meet or exceed designer specified combination of macroscale properties or performance criteria [Fullwood et al. (2009); Adams et al. (2001); Kalidindi et al. (2004); Houskamp et al. (2007); Knezevic and Kalidindi (2007); Knezevic et al. (2008)]).

The critical need to couple physical phenomena occurring over several length scales demands concurrent execution of sophisticated numerical models within other sophisticated numerical models in a hierarchical manner. Computationally efficient strategies to accomplish this arduous task do not exist currently. Moreover, the need for potential inversion of information flow in these models to address materials design problems demands a completely new approach to establishing the MKS. High performance data-mining tools are critically needed for harvesting efficiently the essential knowledge contained in the very large experimental and modeling datasets being produced by experts in the materials related fields. There should be tremendous benefits to treating the very large datasets produced by materials researchers as digital signals, and applying established methods in Signal Processing and Systems Engineering to extract the underlying MKS. It is noteworthy that modern approaches to understanding structure-property-processing relationships have strong analogues in non-linear system theory and informatics.

The central tenet of the novel approach suggested here by the authors is that MKS should necessarily capture the localization information at the lower length scale, as opposed to just establishing the correlations between the macroscale properties and ensemble averaged microstructure statistics. Note that the later constitute only a small subset of the former. In other words, MKS should constitute the *local*

structure-response-structure evolution correlations. Local response refers to the localization of the imposed loading conditions. For example, in mechanical design problems, the essential knowledge systems we seek should describe how the imposed loading at the higher length scale is distributed at the lower length scale. This localization is expected to be strongly correlated to the details of the local structure in the material. MKS should also capture the details of the associated changes in the local structure (referred to as the local structure evolution) which are again expected to be strongly correlated to the details of the local structure.

The main purpose of this paper is to introduce a novel computationally efficient framework for building MKS that is largely based on established concepts in systems theory. After introducing the framework in Section 2, we demonstrate its viability in Section 3 through two selected example case studies involving very different nonlinear physical phenomena: (i) rigid-plastic deformation of a two-phase composite, and (ii) spinodal decomposition of a binary alloy. We present concluding remarks in Section 4.

2 Novel Framework for Materials Knowledge Systems

We start with a discrete representation of the microstructure consistent with the datasets produced by modern materials characterization equipment. We assume that the spatial domain of the material internal structure is binned into a uniform grid of spatial cells (or voxels) that are enumerated by a three-dimensional vector $\mathbf{s}$ whose components take only integer values. Let $\mathbf{S}$ and $|\mathbf{s}|$ represent the complete set of all spatial cells and the total number of spatial cells, respectively, in the given dataset. The microstructure datasets typically identify the local state in each cell. The set of all distinct local states that are possible in a given material system is referred to as the local state space. In this work, the local state space of interest is also assumed to be tessellated into individual bins and enumerated by $h=1,2,\ldots,H$. The variable $m_{\mathbf{s}}^h$ then defines the volume fraction of local state h in the spatial cell $\mathbf{s}$. Based on this definition of the discretized microstructure variable, it is easy to establish the following properties [Adams et al. (2005)]:

$$\sum_{h=1}^{H} m_{\mathbf{s}}^h = 1, \quad m_{\mathbf{s}}^h \geq 0, \quad \frac{1}{|\mathbf{S}|}\sum_{\mathbf{s}\in\mathbf{S}} m_{\mathbf{s}}^h = V^h \tag{1}$$

where V^h denotes the volume fraction of local state h in the complete microstructure dataset.

Let $\mathrm{p}_{\mathbf{s}}$ denote the local response variable in the spatial bin of interest, $\mathbf{s}$. This could represent any local response of interest such as stress, strain, or strain rate. Let $\bar{\mathrm{p}}$ represent the volume averaged value of the response for the entire microstructure.

Drawing on analogues in systems theory [Tong (1995); Boyd and Chua (1985); Nikias and Petropulu (1993)], the localization of the response variable in the microstructure can be expressed as a series of higher-order convolutions involving the microstructure signal and the response signal as

$$\frac{p_{\mathbf{s}}}{\overline{p}} = \left(\sum_{h=1}^{H} \sum_{\mathbf{t} \in \mathbf{S}} \alpha_{\mathbf{t}}^{h} m_{\mathbf{s}+\mathbf{t}}^{h} + \sum_{h=1}^{H} \sum_{h'=1}^{H} \sum_{\mathbf{t} \in \mathbf{S}} \sum_{\mathbf{t}' \in \mathbf{S}} \alpha_{\mathbf{t}\mathbf{t}'}^{hh'} m_{\mathbf{s}+\mathbf{t}}^{h} m_{\mathbf{s}+\mathbf{t}+\mathbf{t}'}^{h'} + \dots \right) \tag{2}$$

Note that in writing Eq. (2) we are treating the spatial distributions of both the microstructure variable and the response variable as digital signals. For example, when we subject a representative volume element (RVE) of a material structure to a specific macroscale loading condition (say tensile stress) and simulate the internal stress field in the RVE using a finite element model, we obtain a very large dataset that can be treated as a digital signal. In current practice, we do not utilize these datasets very efficiently. Often, we extract only a limited number of predictions (e.g. effective macroscale properties, hot spots in stress fields) and throw away much of the rest of the information contained in the dataset. However, there exist underlying correlations (i.e. knowledge) implicit in these datasets that would efficiently capture the underlying physics in the system. Such correlations should be local for a given boundary condition. In other words, for a given loading condition, the stress at a selected spatial point should depend primarily on the details of the structure in a certain neighbourhood of that point – let us call this neighbourhood as the influence zone. Eq. (2) expresses the local interactions in the influence zone as a series sum. Although Eq. (2) was established based on analogues in systems theory, it is gratifying to note that the exact same expression can be derived following the statistical continuum mechanics theories developed by Kroner [Kroner (1986); Binci et al. (2008); Kalidindi et al. (2008)].

In Eq. (2), $\alpha_{\mathbf{t}}^{h}$ and $\alpha_{\mathbf{t}\mathbf{t}'}^{hh'}$ are referred to as the first-order and second-order influence coefficients, respectively, and constitute the materials knowledge system (MKS) described earlier. The values of these coefficients are expected to be completely independent of the microstructure coefficients $m_{\mathbf{s}}^{h}$. $\alpha_{\mathbf{t}}^{h}$ captures the influence of the placement of the local state h in a spatial location that is $\mathbf{t}$ away from the spatial cell of interest denoted by $\mathbf{s}$. In this notation, the components of $\mathbf{t}$, like $\mathbf{s}$, are also integers. The microstructure description $m_{\mathbf{s}}^{h}$ is assumed to be periodic. Consequently, spatial locations $\mathbf{s}+\mathbf{t}$ that lie outside the given microstructure dataset have equivalent identical locations within the given dataset. Figure 1 further clarifies the physical interpretation of the influence coefficients defined in Eq. (2). By extension, the second-order influence coefficient $\alpha_{\mathbf{t}\mathbf{t}'}^{hh'}$ captures the additional contribution (over the first-order contribution) with the simultaneous placement of local state h' in spatial cell $\mathbf{s}+\mathbf{t}+\mathbf{t}'$, in addition to placing h in spatial cell $\mathbf{s}+\mathbf{t}$.

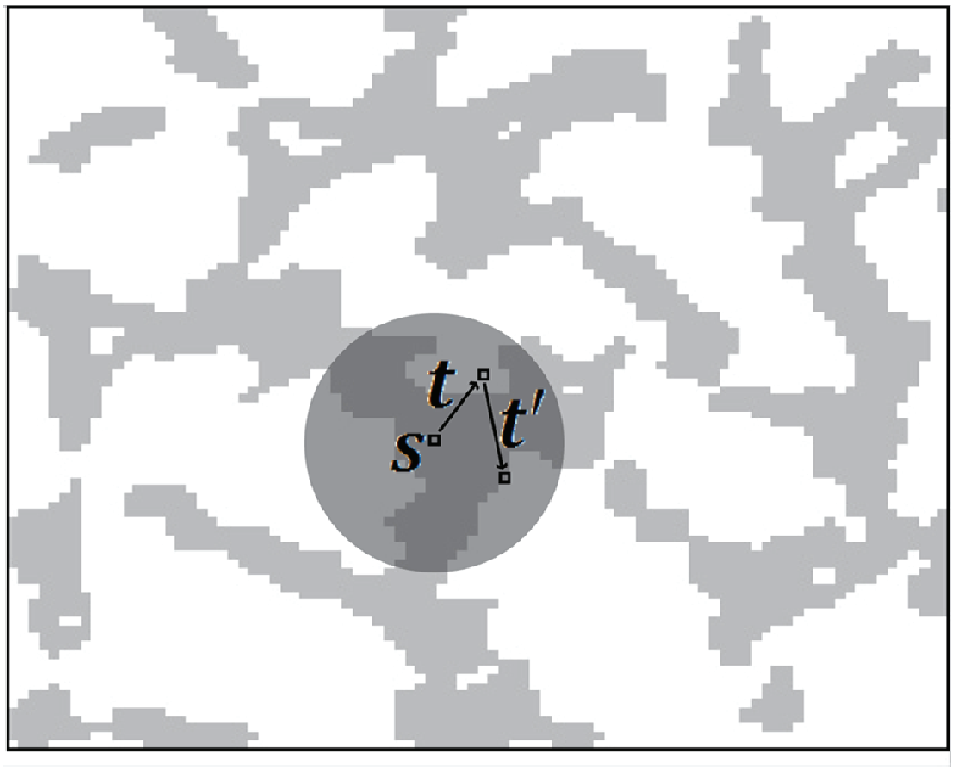

Figure 1: The first-order influence coefficients $\boldsymbol{\alpha}_{\mathbf{t}}^{h}$ capture the contribution to the field variable of interest in spatial cell $\mathbf{s}$ from the placement of local state h in spatial bin $\mathbf{s}+\mathbf{t}$. Likewise, $\boldsymbol{\alpha}_{\mathbf{tt}'}^{hh'}$ captures the contribution from placement of h and h' in spatial bins $\mathbf{s}+\mathbf{t}$ and $\mathbf{s}+\mathbf{t}+\mathbf{t}'$, respectively. The shaded region schematically depicts the influence zone, i.e. microstructure details of the spatial cells outside the influence zone are not expected to influence the localization of the imposed variable in the spatial bin of interest, $\mathbf{s}$.

In many ways, the influence coefficients $\alpha_{\mathbf{t}}^{h}$ are analogous to Green's functions used in mechanics [Roach (1982)]. Green's functions capture the displacement caused by a unit load placed at a certain distance from the location of interest. In the same way, the influence coefficients $\alpha_{\mathbf{t}}^{h}$ capture the contribution to the field variable of interest arising from placement of local state, h, at a spatial location $\mathbf{t}$ away from the point of interest in the microstructure. Just like the Green's functions, we expect $\alpha_{\mathbf{t}}^{h} \rightarrow 0$ as $\mathbf{t}$ takes on large values (larger than the size of the influence zone). This feature will be of tremendous value in analyzing the very large microstructure

datasets produced by modern materials characterization equipment. For example, Synchrotron radiation micro-tomography routinely yields microstructure datasets containing 2000 X 2000 X 2000 voxels [Breidenbach (2009)]. These large microstructure datasets are not amenable to analyses using voxel-based finite element meshes, because of the excess demands they place on computational resources. However, because of the finite size of the influence zone, it becomes feasible to apply Eq. (2) on very large microstructure datasets (details of the computations will become apparent later).

The main challenge with Eq. (2) is the estimation of the numerical values of the influence coefficients $\alpha_{\mathbf{t}}^{h}$. The traditional approach for establishing the values of influence coefficients in the framework of the statistical continuum theories is to derive analytical expressions for the series expansion [Adams and Olson (1998); Kroner (1986); Binci et al. (2008); Kalidindi et al. (2008); Garmestani et al. (1998, 2001); Beran (1968)]. This is accomplished by invoking a hypothetical reference medium and transforming the governing equations to an equivalent problem in a homogeneous reference medium subjected to a fictitious loading condition. The main drawbacks of this approach have been the following: (i) the accuracy of the predictions is very sensitive to the choice of a reference medium that is often restricted to an isotropic reference due to complexity of the computations involved, and (ii) the high complexity associated with numerical evaluation of the convolution integrals involved (the integrand exhibits a singularity in the domain of integration; also called principal value problem). Although a number of advances have been made in addressing these complex issues [Kalidindi et al. (2006); Fullwood et al. (2008); Torquato (1997)], these theories have not yet attained the desired accuracy in predicting the internal stress and strain fields in the composite microstructures.

In recent work, the authors and their collaborators have demonstrated that it might be possible to establish much more accurate localization relationships by calibrating the series expansions of Eq. (2) to results obtained from finite element (FE) models [Binci et al. (2008); Kalidindi et al. (2008)]. The main difficulty with Eq. (2) is that all of the influence coefficients are fully coupled. A logical approach to establishing the influence coefficients in Eq. (2) is to consider one set of terms at a time. In other words, we could consider initially only the first-order terms, develop a scheme to establish all of the first-order coefficients $\alpha_{\mathbf{t}}^{h}$, define a residual error field that persists after accounting for the first-order terms, use the residual error field to calibrate all of the second-order coefficients, and so on. It should be noted that the calibration task gets progressively more difficult. Based on Eq. (2), the total number of first-order influence coefficients is $|\mathbf{S}|H$, while the total number of second-order influence coefficients is $(|\mathbf{S}|H)^2$. It is seen that the num-

ber of influence coefficients increases dramatically with the higher-order terms. It should be noted that the number of first-order influence coefficients is itself quite substantial for most microstructure datasets, because $|\mathbf{S}|$ is typically very large. The focus in this work will be mainly on the first-order terms, although we will present the framework in the most generalized form and hint at some future strategies for estimating the higher-order influence coefficients.

Even considering only the first-order coefficients, their numbers are extremely large to allow calibration with FE results using any of the standard linear regression analyses methods. Therefore, in prior work [Binci et al. (2008); Kalidindi et al. (2008)], we were forced to restrict our considerations to only the first-neighbours in calibrating the influence coefficients to FE results. The main contribution of the present work is the recognition that Eq. (2) takes a much simpler form when transformed into the discrete Fourier transform (DFT) space, where it can be recast as

$$P_{\mathbf{k}} = \left[\left(\sum_{h=1}^{H} \beta_{\mathbf{k}}^{h*} M_{\mathbf{k}}^{h} \right) + \left(\sum_{h=1}^{H} \sum_{h'=1}^{H} \sum_{\mathbf{r}?\mathbf{s}} \beta_{\mathbf{k}r}^{hh'*} M_{\mathbf{r}}^{h'} M_{\mathbf{k}-\mathbf{r}}^{h} \right) + \ldots \right] \tag{3}$$

$$\beta_{\mathbf{k}}^{h} = \Im_{\mathbf{k}} \left(\alpha_{\mathbf{t}}^{h} \right), \qquad P_{\mathbf{k}} = \Im_{\mathbf{k}} \left(\mathrm{p_s}/\overline{\mathrm{p}} \right), \qquad M_{\mathbf{k}}^{h} = \Im_{\mathbf{k}} \left(m_{\mathbf{s}}^{h} \right) \tag{4}$$

where $\Im_{\mathbf{k}}(\ )$ denotes the multi-dimensional DFT operation (three-dimensional for 3-D datasets with the DFT taken in each dimension separately) with respect to the spatial variables $\mathbf{s}$ or $\mathbf{t}$, and the star in the superscript denotes the complex conjugate. The simplification in Eq. (3) compared to Eq. (2) is a direct consequence of well-known convolution properties of DFTs [Oppenheim et al. (1999)]. Note that the number of coupled first-order coefficients in Eq. (3) is only H, although the total number of first-order coefficients still remains as $|\mathbf{S}|H$. Because of this dramatic uncoupling of first-order coefficients into smaller sets, it becomes fairly easy to estimate the values of influence coefficients $\beta_{\mathbf{k}}^{h}$ by calibrating them to results from FE models.

It is emphasized here that establishing $\beta_{\mathbf{k}}^{h}$ is a one-time computational task for a selected composite material system, because these coefficients are expected to be independent of the morphology of the microstructure (defined by $m_{\mathbf{s}}^{h}$). As such, they offer a compact representation of the underlying knowledge regarding the localization of the selected response variable for all possible topologies that could be defined in the given composite material system. The simplicity of Eq. (3) also presents a computationally efficient procedure for computing the spatial distribution of the selected response variable for any microstructure dataset, after the corresponding influence coefficients are established and stored. However, it should be noted that the influence coefficients are expected to be strongly dependent on

the imposed boundary conditions, i.e. they need to be established separately for all boundary conditions of interest. Strategies for expressing the functional dependence of the influence coefficients on the imposed boundary conditions will be discussed in the context of the specific case studies selected later.

The estimation of the second-order influence coefficients is beyond the scope of the present work. However, it is pointed out that there exist several established methods in digital signal processing for estimating these influence coefficients (e.g. Volterra series [Ogunfunmi (2007)]). All of the discussion above was focused on the local structure-response correlations. For local structure-structure evolution correlations, we essentially use the same approach (i.e. Eqs. (2)–(4)) and simply replace the local response variable, p_s, with the appropriate local structure evolution variable. This will be exemplified later with a specific case study.

Before closing this section, we bring to the reader's attention the fact that the redundancies expressed in Eq. (1) make it impossible to establish independently all of the values of the influence coefficients, $\alpha_{\mathbf{t}}^{h}$. In fact the $|\mathbf{S}|$ redundancies in Eq. (1), reduce the number of independent influence coefficients from $|\mathbf{S}|H$ to $|\mathbf{S}|(H\text{-}1)$. So it becomes necessary to either recast Eqs. (2)–(4)) in terms of the independent influence coefficients or to utilize reduced-rank methods based on singular value decomposition (SVD) or principal component analysis [Izenman (1975); Davies and Tso (1982)]. In our work, we have applied both strategies and obtained identical results.

3 Case Study I: Rigid-Plastic Deformation of a Two-Phase Composite

3.1 Physics of the Phenomenon

In this example, we present the application of the framework described above to the rate-independent rigid-plastic deformation of a two-phase representative volume element (RVE), with no strain hardening. The two phases are assumed to exhibit isotropic plasticity with yield strengths of 200 MPa and 250 MPa, respectively. The stress-strain relationships for both phases are assumed to be described by the Levy-Mises equations [Khan and Huang (1995)] as

$$\boldsymbol{\varepsilon} = \lambda \boldsymbol{\sigma}' \tag{5}$$

where $\dot{\boldsymbol{\varepsilon}}$ is the symmetric strain rate tensor, $\boldsymbol{\sigma}'$ is the symmetric deviatoric Cauchy stress tensor, and λ is a proportionality parameter that can be related to the yield strength of the material, the equivalent plastic strain rate and the equivalent stress. Although it is not directly apparent from Eq. (5), the constitutive relation described implies a rate-independent plastic response. The goal of the localization expression

in this example is to compute the local strain rate field in the RVE of the two-phase composite. For simplicity, we initially demonstrate the establishment of the localization relationship for the case of an applied isochoric simple compression strain rate tensor on the RVE at the macroscale, with equal extension in lateral directions, expressed as

$$\dot{\bar{\boldsymbol{\varepsilon}}}_{ij} = \begin{bmatrix} \dot{\bar{\varepsilon}} & 0 & 0 \\ 0 & -0.5\dot{\bar{\varepsilon}} & 0 \\ 0 & 0 & -0.5\dot{\bar{\varepsilon}} \end{bmatrix} \tag{6}$$

We will subsequently discuss the extension of this localization relationship for other imposed strain rate tensors.

3.2 Microstructure Variables and Local State Space

For this example, the local state space is comprised of two isotropic phases (*H=2*), where *h=1* identifies the first local state (phase) and *h=2* the second one. We assume each cell of the tessellated spatial domain to be completely filled with either of the two local states (see Figure 1). Thus, the microstructure variable $m_{\mathbf{s}}^{h}$ takes on values of zeros or ones. For instance, if a given cell $\mathbf{s}$ is occupied by the first phase, then $m_{\mathbf{s}}^{1} = 1$ and $m_{\mathbf{s}}^{2} = 0$.

3.3 First-Order Localization Relationship

Based on Eqs. (3) and (4), the first-order localization linkage for the present problem can be expressed in the DFT space as

$$\mathfrak{F}_{\mathbf{k}}(\dot{\varepsilon}_{\mathbf{s}}) = \left[\sum_{h=1}^{H=2} \beta_{\mathbf{k}}^{h*} M_{\mathbf{k}}^{h} \right] \dot{\bar{\varepsilon}}, \tag{7}$$

where $\dot{\boldsymbol{\varepsilon}}_{\mathbf{s}}$ represents the local strain rate tensor in the spatial bin $\mathbf{s}$, and $\dot{\bar{\varepsilon}} = 0.02s^{-1}$ is the macroscopically imposed strain rate in the $\mathbf{e}_1$ direction on the RVE (see Eq. (6)). It is also important to note that in the notation used in Eq. 11, both $\dot{\boldsymbol{\varepsilon}}_{\mathbf{s}}$ and $\boldsymbol{\beta}_{\mathbf{k}}^{h*}$ are second-rank tensors. Introducing the constraints of Eq. (1) into Eq. 6 results in

$$\mathfrak{I}_{\mathbf{k}\neq\mathbf{0}}(\dot{\boldsymbol{\varepsilon}}_{\mathbf{s}}) = \left[\left(\boldsymbol{\beta}_{\mathbf{k}}^{1*} - \boldsymbol{\beta}_{\mathbf{k}}^{2*} \right) M_{\mathbf{k}}^{1} \right] \dot{\bar{\varepsilon}} = \left[\boldsymbol{\gamma}_{\mathbf{k}}^{1} M_{\mathbf{k}}^{1} \right] \dot{\bar{\varepsilon}} \tag{8}$$

$$\mathfrak{I}_{\mathbf{0}}(\dot{\boldsymbol{\varepsilon}}_{\mathbf{s}}) = |\mathbf{s}| \left(\dot{\bar{\varepsilon}} \mathbf{e}_1 \bigotimes \mathbf{e}_1 - 0.5\dot{\bar{\varepsilon}} \mathbf{e}_2 \bigotimes \mathbf{e}_2 - 0.5\dot{\bar{\varepsilon}} \mathbf{e}_3 \bigotimes \mathbf{e}_3 \right) \tag{9}$$

Eq. (9) simply indicates that the macroscopic strain rate on the RVE is the same as volume averaged strain rate from the microscale. This happens to be true for

the case study selected here. For other phenomena where this requirement does not hold, additional attention needs to be paid in setting up Eq. (9) and may need s to be modified appropriately with the use of higher-order terms in the series.

It is also important to recognize that if the $\boldsymbol{\gamma}_{\mathbf{k}}^{\mathbf{l}}$ are known, the local strain rate field for any given microstructure dataset $m_{\mathbf{s}}^{h}$ subjected to the simple compression loading condition selected here can be computed by applying Eqs. (8) and (9) and performing a simple inverse DFT.

3.4 Calibration of Influence Coefficients

As described earlier, the values of $\boldsymbol{\gamma}_{\mathbf{k}}^{\mathbf{l}}$ are established by regression analysis using datasets produced by FE models on selected microstructures. In our work, we discovered that "delta" microstructures, consisting of one element of one phase surrounded completely by another phase, are very convenient for the calibration process and produce the best estimates for $\boldsymbol{\gamma}_{\mathbf{k}}^{\mathbf{l}}$. In a two-phase composite, it is possible to define only two distinct delta microstructures, and both of these were used in the calibration process for this problem. This selection is also motivated by the recognition that Eqs. (8) and (9) represent a linear and space-invariant causal system. For such systems, when the output for an impulse (i.e. delta microstructure) is known, thean the output for any other microstructure input can be described as a convolution of the input with the impulse response [Oppenheim et al. (1999)]. All of the FEM results used in this study were generated using the commercial software ABAQUS®, where each RVE contained 804,357 (93x93x93) cuboid-shaped three-dimensional eight-noded solid elements. The use of cube-shaped elements naturally defines a regularly spaced grid, conducive to the computation of the DFTs. The macroscale simple compression strain rate was imposed on the finite element mesh as a periodic uniform boundary condition. The values of $\boldsymbol{\gamma}_{\mathbf{k}}^{\mathbf{l}}$ were established as the best-fit values for the FE results on the two delta microstructures described above, using standard linear regression analyses methods [Montgomery et al. (2006)].

3.5 Validation of the MKS

The established $\boldsymbol{\gamma}_{\mathbf{k}}^{\mathbf{l}}$ coefficients constitute the *materials knowledge systems* (MKS) for the case study presented. In fact, the strain rate field for any other RVE comprising any spatial arrangements of the same constituent phases, subjected to the same simple compression loading condition, can be easily computed using Eqs. (8) and (9). As a critical validation of this concept, we explore the application of the MKS established here to a random microstructure of the selected two phases. We selected a random microstructure for our validation here because their rich diversity of local neighbourhoods produce the most heterogeneous microscale strain rate fields in the

composite, and therefore offer an excellent opportunity to evaluate the localization relationships most critically. We note that we have successfully applied the MKS developed here to a large number of microstructures, although only one example is described here in detail. Figure 2 compares the local $\dot{\varepsilon}_{11}$ component of the strain rate field for the selected random microstructure using both the FE analysis and the MKS approach developed in this work.

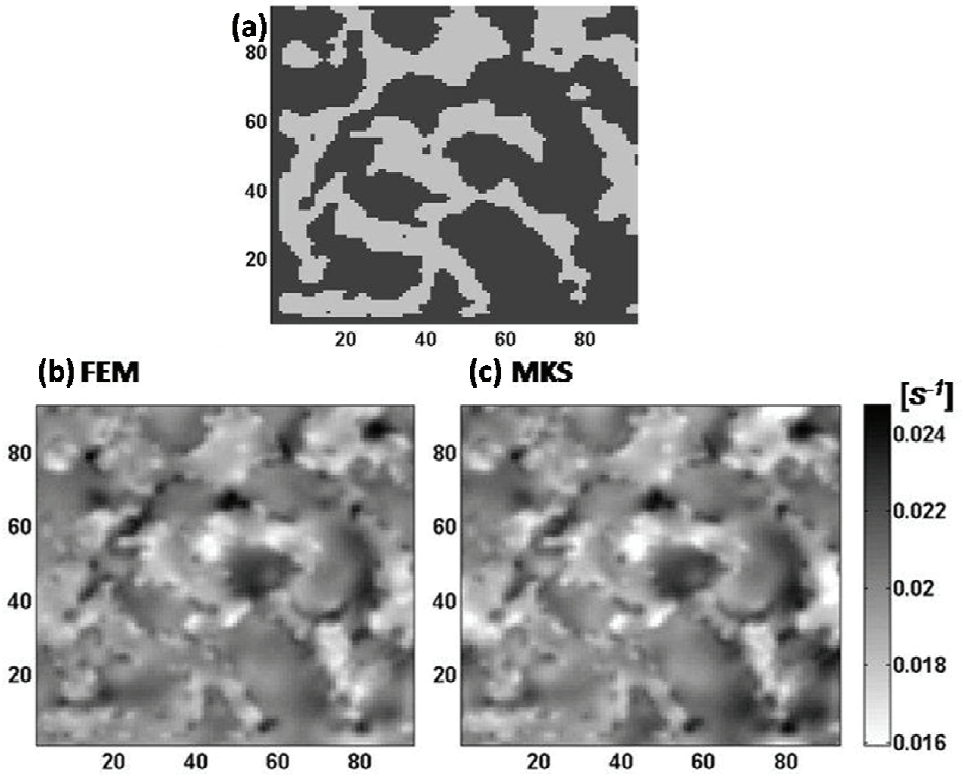

Figure 2: Comparison of the contour maps of the local $\dot{\varepsilon}_{11}$component of the strain rate tensor for a 3-D microstructure. The middle section of the 3-D RVE used in the calculation is shown at the top (a), while the predicted strain rate contours by the FE method (b) and the MKS established in this work (c) are shown below. Both phases are assumed to exhibit isotropic plasticity with yield strengths of 200 MPa and 250 MPa, respectively. The macroscopic simple compression strain rate applied is 0.02 s^{-1}.

The error between the predictions shown in Figure 2 from the MKS approach de-

scribed here and the FEM analysis can be quantified in each spatial bin as

$$Err_{\mathbf{s}} = \left| \frac{((\dot{\varepsilon}_{11})_{\mathbf{s}})_{FEM} - ((\dot{\varepsilon}_{11})_{\mathbf{s}})_{MKS}}{\bar{\dot{\varepsilon}}_{11}} \right| \times 100 \tag{10}$$

where the subscripts FEM and MKS indicate that the predictions were made using FEM and MKS Methods, respectively. Based on the above definition, the average value of $Err_{\mathbf{s}}$ over all of the spatial bins for the microstructure shown in Figure 2 is only 2.2%. The FE analyses could not be performed on a regular desktop PC. It was executed on an IBM e1350 supercomputing system (part of The Ohio Supercomputer Center), and required 94 processor hours. In contrast, the MKS method took only 32 seconds on a regular laptop (2GHz CPU and 2GB RAM).

3.6 Other Considerations

In the present case study, MKS was developed for a very specific loading condition (i.e. simple compression strain rate tensor). In order to extend the MKS presented here to general loading conditions, we need substantially more effort. Although such an extension is beyond the scope of the present study, we outline below a strategy to address this challenge. Towards this end, Eq. (11) could be generalized as

$$mathfrakF_{\mathbf{k}}(\dot{\varepsilon}_{\mathbf{s}}) = \sum_{h=1}^{H=2} \beta_{\mathbf{k}}^{h*}(\bar{\dot{\varepsilon}}) m_{\mathbf{k}}^{h} \tag{11}$$

where the dependence of $\boldsymbol{\beta}_{\mathbf{k}}^{h}$ on the macroscale imposed strain rate tensor, $\bar{\dot{\boldsymbol{\varepsilon}}}$, is explicitly noted. We therefore need to establish the functional dependence of $\boldsymbol{\beta}_{\mathbf{k}}^{h}$ in the space of symmetric second rank tensors, which is a six-dimensional space. However, if we elect to solve the problem in the principal frame of $\bar{\dot{\boldsymbol{\varepsilon}}}$ (i.e. the microstructure signal needs to be appropriately rotated), then the domain of interest for describing $\boldsymbol{\beta}_{\mathbf{k}}^{h}$ reduces to a three-dimensional space. If we further exploit the fact that the magnitude of $\bar{\dot{\boldsymbol{\varepsilon}}}$ has no effect on the localization (a consequence of the rate-independence of the plastic response) and we require $\bar{\dot{\boldsymbol{\varepsilon}}}$ to be traceless (to reflect volume conservation during plastic deformation), then the domain of interest for describing $\boldsymbol{\beta}_{\mathbf{k}}^{h}$ can be expressed using a single angular variable [Van Houtte (1994); Knezevic et al. (2009)]. The functional dependence of $\boldsymbol{\beta}_{\mathbf{k}}^{h}$ on this single angular variable can be expressed conveniently using DFTs following the approach outlined in our earlier work [Knezevic et al. (2009)].

As a final comment on this case study, we point out that the composite material studied here had only a low contrast (yield strength ratio 1.25) in the properties of the constituent phases (i.e. the yield strengths were 200 MPa and 250 MPa,

respectively). Based on the various case studies we have successfully completed, it is clear that the first-order influence coefficients provide good predictions for composites with low and moderate contrasts. With moderatre (yield strength ratio >3-5) or even higher contrasts (yield strength ratio >10) in the properties of the constituents, it is imperative to include the second-order term shown in Eq. (3).

4 Case Study II: Spinodal Decomposition of a Binary Alloy

4.1 Physics of the Phenomenon

Spinodal decomposition [Cahn (1961)] is a phase transformation where a homogenous mixture separates into regions of distinct chemical composition or phase. Unlike most phase transformations in solids there is no thermodynamic barrier to the separation, spinodal decomposition occurs completely by a diffusion clustering mechanism, assisted by a negative energy gradient in free energy. This driving force is modulated by the energy cost of creating an interface between the phase separated regions. Phase separation by spinodal decomposition of a binary alloy into two phases, denoted a and b, can be described by the well known Cahn-Hilliard equation as [Cahn and Hilliard (1958); Novick-Cohen and Segel (1984)]

$$\dot{c} = \nabla^2 D(c) \left(\frac{df(c)}{dc} - K\nabla^2 c \right), \tag{12}$$

where c is a conserved order parameter describing the atomic fraction of phase b at a given spatial point. $f(c)$ is the free energy as a function of c, D is a diffusion coefficient, and K is a property of the interface created by the phase separation. The functional dependence of free energy on c is generally assumed to be a classic double-well potential [Cahn (1961)], and is often approximated with a 4th-order polynomial as

$$f(c) = 4F\left(c^2 - 1\right)^2, \tag{13}$$

where F is the height of the energy barrier between the two minima. Note that $f(c)$ has global minima at $c = 0$ and $c = 1$.

4.2 Microstructure Variables and Local State Space

For this example, the local state is in actuality adequately described by a single variable, c. However, in developing the MKS, we found it much more convenient to include $\frac{df}{dc}$ as an additional local state variable. Although c and $\frac{df}{dc}$ are related to each other by Eq. (13), the mapping from $\frac{df}{dc}$ to c is not unique. Since the details of structure evolution in this case study are strongly dependent on the spatial variation

of $\frac{df}{dc}$, we found it advantageous to include it in the description of the local state as an additional parameter. Consequently, unlike the plasticity example where the local state space was discrete, the local state space here is continuous and two-dimensional (in the shape of a rectangle).

Our strategy in developing MKS for this case study would be to seek an appropriate binning of the local state space. In the simple demonstration of our framework presented here, we have defined four local states, indexed 1 thru 4, corresponding to the corners of the rectangular-shaped local state space (i.e. the space identifying all of the feasible combinations of c and $\frac{df}{dc}$). Any feasible local state can then be thought of as a linear weighted combination of the local states $h = 1$ through $h = 4$. Thus the microstructure variable $m_{\mathbf{s}}^h$ takes continuous values between 0 and 1, reflecting the volume fraction of each of the selected corner local states. Also note that $H = 4$ for the selected idealization.

It is possible to frame this problem using only c as the local state of interest. Note however that Eq. 13 is nonlinear in c with explicit dependence on both c and $\frac{df}{dc}$. By defining the local state over both parameters, we are reducing the problem to a linear system. It is expected (and will be demonstrated below) that the first order terms in the MKS will fully capture the resulting local structure-structure evolution linkages.

4.3 First-Order Localization Relationship

Following the same approach presented earlier for the plasticity case study, the reduced first-order microstructure evolution linkage can be expressed in the DFT space as (see Eqs. (8) and (9))

$$\mathfrak{I}_{\mathbf{k}\neq\mathbf{0}}\left(\dot{c}_{\mathbf{s}}\right) = \sum_{h=1}^{3} \gamma_{\mathbf{k}}^{h*} M_{\mathbf{k}}^{h}, \quad \mathfrak{I}_{\mathbf{0}}\left(\dot{c}_{\mathbf{s}}\right) = 0 \tag{14}$$

where $\dot{c}_{\mathbf{s}}$ is the time rate of change in c in spatial bin $\mathbf{s}$. Note that the order parameter c is conserved, and that the average of $\dot{c}_s$ over the RVE is identically zero. Thus the form of Eq. (14) is slightly different than Eqs. (8) and (9) in that there is no macroscopically applied term. Also in this case both $\dot{c}_s$ and the coefficients $\gamma_{\mathbf{k}}^{h*}$ are scalars. As in the previous example, once the $\gamma_{\mathbf{k}}^{h}$ are known, $\dot{c}_s$ can be readily computed for any microstructure, $m_{\mathbf{s}}^h$, using Eq. (14) and performing the inverse DFT. The microstructure can then be evolved by any suitable time integration method. In this work, we used a simple Euler forward scheme.

4.4 Calibration of Influence Coefficients

In the previous example, the materials knowledge system was calibrated to FE models. For the present case study, we established the MKS by calibrating Eq. (14) to

results from a phase field model (Courtesy of Yunzi Wang, The Ohio State University) that has been previously demonstrated to successfully simulate the separation of a binary alloy via spinodal decomposition. Generally, the initial conditions for the phase field simulations are a uniform field perturbed from equilibrium by a Langevin Noise [Lax (1966)], and the boundary conditions are prescribed to maintain the assumed periodicity of the structure. One such simulation was performed on a 1000x1000 grid with a time step of $\triangle t = 0.2s$ until a final time of 400s, at which time the system is completely phase separated. The fields c_s , $\left(\frac{df}{dc}\right)_s$, and $\dot{c}_s$ were stored at the initial, final and two intermediate time steps as shown in Figure 3. These datasets were used to calibrate the influence coefficients in Eq. (14) using standard linear regression analysis methods [Montgomery et al. (2006)].

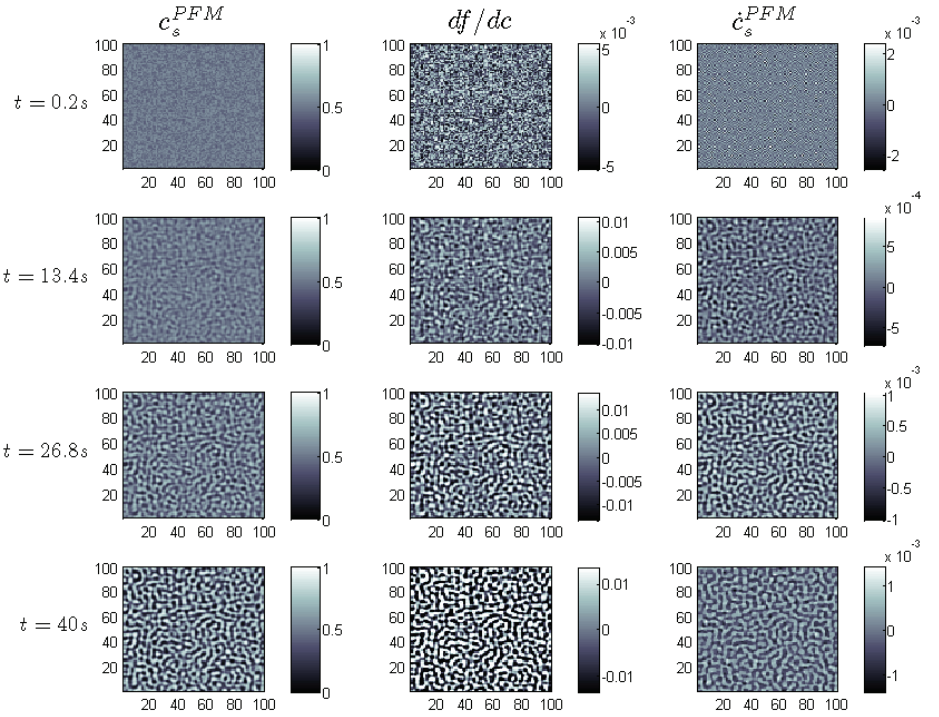

Figure 3: Datasets obtained at selected times in the evolution of a specific phase field simulation that were used in the calibration of the influence coefficients.

4.5 Time Integration

Since MKS described above produces a linkage between the time rate of change in the structure variable (see Eq. (14)), we need to select an appropriate time integration scheme to update the structure at the end of a given time step, so that we can effectively march forward in time. In the present work, we employed a simple Euler forward scheme expressed as

$$c_{\mathbf{s}}(t+\triangle t) = c_{\mathbf{s}}(t) + \triangle t \dot{c}_{\mathbf{s}}. \tag{15}$$

Once the microstructure is updated, time is reset to $t = t + \triangle t$, and this process is repeated until the desired final time is reached. The same time step that was used in the phase field model was used with the MKS method.

4.6 Validation of the MKS

For validation of the MKS developed here, we simulated spinodal decomposition in the same material system (i.e. same values of materials parameters *D, K*, and *F*; see Eqs. (12) and (13)) with different initial microstructures (i.e. different perturbations from equilibrium by a Langevin Noise [Lax (1966)]). In all of the examples we tested, the predictions from MKS matched exactly with the corresponding predictions from Phase-field models, keeping errors within machine precision levels. Figure 4 shows a comparison for one such validation example, where we directly compare the conserved field predicted by MKS with the corresponding prediction from phase-field models. The local error in the predicted conserved field variable at any spatial point in the RVE in the entire simulation was on the order of machine precision (less than 1×10^{-12}). The computational time savings for this class of problems was observed to be about a factor of two in favour of the MKS method.

4.7 Other Considerations

The MKS system developed for the spinodal decomposition case study produced significantly lower level of computational savings compared to the earlier case study on plastic deformation. This is mainly because the governing equations in this case study are relatively simple. We should see significant savings in the MKS method when the governing equations are complex and require a large number of computations at each time step (solving a set of stiff nonlinear equations as in the case of plasticity case study). Even though we attained only a modest computational advantage for this case study, it is worth remembering that the MKS approach can be applied to much larger datasets compared to the phase-field approach. This is mainly because of the localization relationship in the MKS that only extends the influence at any spatial location to a finite neighbourhood. Also

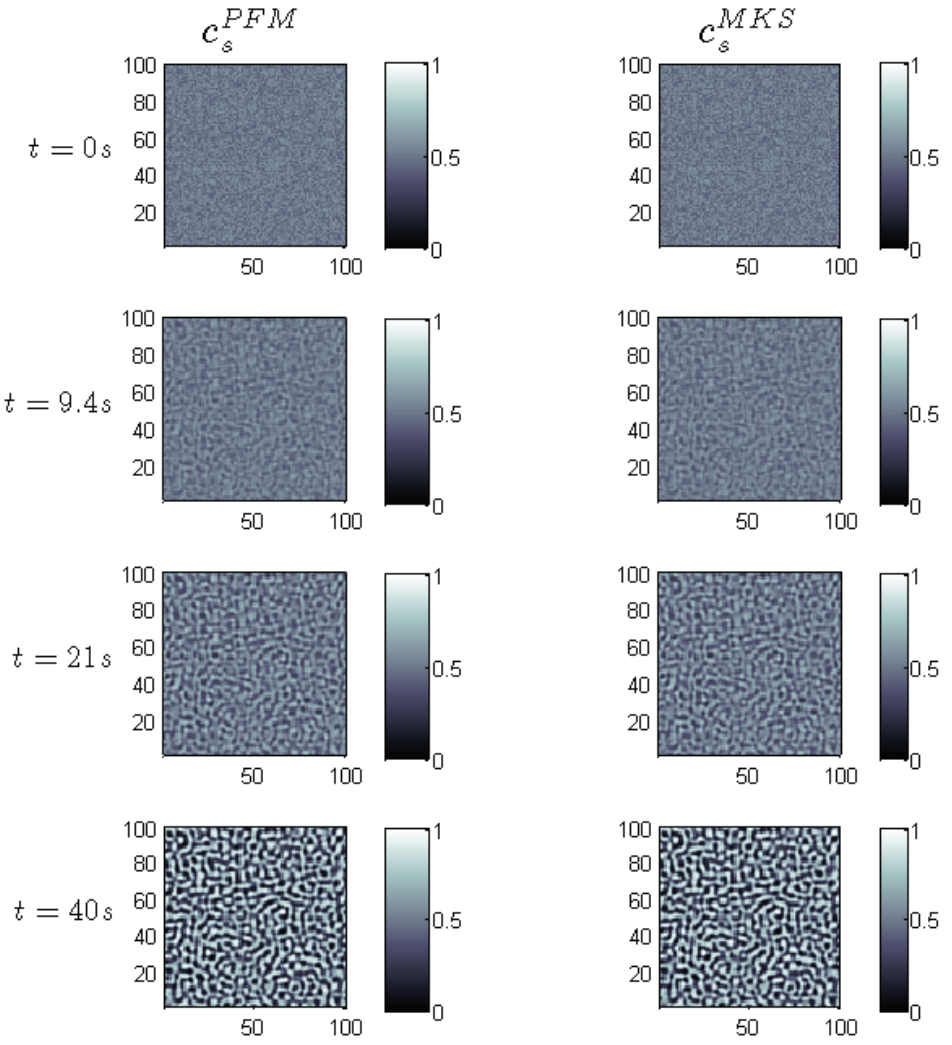

Figure 4: A comparison between the predicted conserved fields from the MKS approach and the phase-field model. The initial field as well as its evolution at various intermediate stages during the spinodal decomposition process are captured in these plots. The maximum discrepancy at any spatial location between the two predictions is less than 1×10^{-12}.

since the localization relationship can be applied to each spatial bin independently, the MKS approach is much more amenable to parallel computations.

5 Conclusions

We have presented a novel mathematical framework for building a comprehensive materials knowledge system (MKS) to extract, store and recall hierarchical structure-property-processing linkages. The framework is very general and can be applied to a broad range of physical phenomena in a broad range of material systems. We have presented novel FFT (Fast Fourier Transforms)-based algorithms for data-mining local structure-response-structure evolution linkages from large numerical datasets produced by established modelling strategies for microscale phenomena. The viability of this new approach was demonstrated with two selected case studies whose governing field equations exhibit a high degree of non-linearity. In both cases, it was noted that the first-order influence coefficients adequately captured the localization relationships in spite of the non-linearity inherent to the phenomena. It was generally observed that the higher-order coefficients are needed with higher contrast in the local response of the constituent local states.

Acknowledgement: The authors acknowledge financial support for this work from the DARPA-ONR Dynamic 3D Digital Structure project, Award No. N00014-0510504 (Program Manager: Dr. Julie Christodoulou). SRN was funded by the NSF Graduate Research Fellowship Program (NSF-GRFP).

References

Adams BL, Olson T. (1998): The mesostructure - properties linkage in polycrystals. *Progress in Materials Science* 43:1.

Adams BL, Gao X, Kalidindi SR. (2005): Finite approximations to the second-order properties closure in single phase polycrystals. *Acta Materialia* 53:3563.

Adams BL, Henrie A, Henrie B, Lyon M, Kalidindi SR, Garmestani H. (2001): Microstructure-sensitive design of a compliant beam. *Journal of the Mechanics and Physics of Solids* 49:1639.

Alkemper J, Voorhees PW. (2001): Quantitative serial sectioning analysis. *Journal of Microscopy* 201:388.

Amodeo RJ, Ghoniem NM. (1990): Dislocation dynamics. I. A proposed methodology for deformation micromechanics. *Physical Review B* 41:6958.

Beran MJ, Mason TA, Adams BL, Olsen T. (1996): Bounding elastic constants of an orthotropic polycrystal using measurements of the microstructure. *Journal of the Mechanics and Physics of Solids* 44:1543.

Beran MJ. (1968): *Statistical Continuum Theories*. John Wiley & Sons, Interscience, New York, NY.

Binci M, Fullwood D, Kalidindi SR. (2008): A new spectral framework for establishing localization relationships for elastic behavior of composites and their calibration to finite-element models. *Acta Materialia* 56:2272.

Boyd S, Chua L. (1985): Fading memory and the problem of approximating nonlinear operators with Volterra series. Circuits and Systems, *IEEE Transactions* on 32:1150.

Breidenbach B. (2009): Phase contrast X-ray tomography of nut and seed shells. submitted.

Blavette D, Bostel A, Sarrau JM, Deconihout B, Menand A. (1993): An atom probe for three-dimensional tomography. *Nature* 363:432.

Bunge HJ. (1993): *Texture analysis in materials science. Mathematical Methods*. Géttingen: Cuvillier Verlag.

Cahn JW. (1961): On spinodal decomposition. *Acta Metallurgica* 9:795.

Cahn JW, Hilliard JE. (1958): Free Energy of a Nonuniform System. I. Interfacial Free Energy. *The Journal of Chemical Physics* 28:258.

Davies PT, Tso MKS. (1982): Procedures for Reduced-Rank Regression. *Journal of the Royal Statistical Society. Series C* (Applied Statistics) 31:244.

Flannery BP, Deckman HW, Roberge WG, D'Amics KL. (1987): Three-Dimensional X-ray Microtomography. *Science* 237:1439.

Fullwood DT, Niezgoda SR, Adams BL, Kalidindi SR. (2009): Microstructure Sensitive Design for Performance Optimization. *Journal of Progress in Materials Science* in press.

Fullwood DT, Adams BL, Kalidindi SR. (2008): A strong contrast homogenization formulation for multi-phase anisotropic materials. *Journal of the Mechanics and Physics of Solids* 56:2287.

Garmestani H, Lin S, Adams BL. (1998): Statistical Continuum Theory for Inelastic Behavior of a Two-phase Medium. *International Journal of Plasticity* 14:719.

Garmestani H, Lin S, Adams BL, Ahzi S. (2001): Statistical Continuum Theory for Large Plastic Deformation of Polycrystalline Materials. *Journal of the Mechanics and Physics of Solids* 49:589.

Gusev AA, Hine PJ, Ward IM. (2000): Fiber packing and elastic properties of a transversely random unidirectional glass/epoxy composite. *Composites Science and Technology* 60:535.

Hall EO. (1951): The Deformation and Ageing of Mild Steel: III Discussion of Results. *Proceedings of the Physical Society. Section B* 747.

Houskamp JR, Proust G, Kalidindi SR. (2007): Integration of microstructure-sensitive design with finite element methods: Elastic-plastic case studies in FCC polycrystals. *International Journal for Multiscale Computational Engineering* 5:261.

Izenman AJ. (1975): Reduced-rank regression for the multivariate linear model. *Journal of Multivariate Analysis* 5:248.

Kalidindi SR, Houskamp JR, Lyons M, Adams BL. (2004): Microstructure sensitive design of an orthotropic plate subjected to tensile load. *International Journal of Plasticity* 20:1561.

Kalidindi SR, Landi G, Fullwood DT. (2008): Spectral representation of higher-order localization relationships for elastic behavior of polycrystalline cubic materials. *Acta Materialia* 56:3843.

Kalidindi SR, Binci M, Fullwood D, Adams BL. (2006): Elastic properties closures using second-order homogenization theories: Case studies in composites of two isotropic constituents. *Acta Materialia* 54:3117.

Kazaryan A, Wang Y, Dregia SA, Patton BR. (2000): Generalized phase-field model for computer simulation of grain growth in anisotropic systems. *Physical Review B* 61:14275.

Khan AS, Huang S. (1995): *Continuum theory of plasticity*. New York: Wiley.

Knezevic M, Al-Harbi HF, Kalidindi SR. (2009): Crystal plasticity simulations using discrete Fourier transforms. *Acta Materialia* 57:1777.

Knezevic M, Kalidindi SR. (2007): Fast computation of first-order elastic-plastic closures for polycrystalline cubic-orthorhombic microstructures. *Computational Materials Science* 39:643.

Knezevic M, Kalidindi SR, Mishra RK. (2008): Delineation of first-order closures for plastic properties requiring explicit consideration of strain hardening and crystallographic texture evolution. *International Journal of Plasticity* 24:327.

Kroner E. (1986): *Statistical Modelling*. Elsevier Science Publishers.

Lax M. (1966): Classical Noise IV: Langevin Methods. *Reviews of Modern Physics* 38:541.

Li J, Van Vliet KJ, Zhu T, Yip S, Suresh S. (2002): Atomistic mechanisms governing elastic limit and incipient plasticity in crystals. *Nature* 418:307.

Li JY, Rogan RC, Ustundag E, Bhattacharya K. (2005): Domain switching in polycrystalline ferroelectric ceramics. *Nat Mater* 4:776.

Maire E, Buffiére JY, Salvo L, Blandin JJ, Ludwig W, Létang JM. (2001): On the Application of X-ray Microtomography in the Field of Materials Science. *Advanced Engineering Materials* 3:539.

Mason TA, Adams BL. (1999): Use of microstructural statistics in predicting polycrystalline material properties. *Metallurgical and Materials Transactions A: Physical Metallurgy and Materials Science* 30:969.

Montgomery DC, Peck EA, Vining GG. (2006): *Introduction to linear regression analysis*. Hoboken, NJ: Wiley-Interscience.

Nikias CL, Petropulu AP. (1993): *Higher-order spectra analysis: a nonlinear signal processing framework*. Englewood Cliffs, N.J.: PTR Prentice Hall.

Novick-Cohen A, Segel LA. (1984): Nonlinear aspects of the Cahn-Hilliard equation. *Physica D: Nonlinear Phenomena* 10:277.

Ogunfunmi T. (2007): *Adaptive Nonlinear System Identification: The Volterra and Wiener Model Approaches*. Springer.

Oppenheim AV, Schafer, R. W., Buck, J.R. (1999): *Discrete time signal processing*. Prentice-Hall.

Petch NJ. (1953): The cleavage strength of Polycrystals. *Journal of the Iron and Steel Institute* 174:25.

Roach GF. (1982): *Green's Functions*. Cambridge University Press.

Saheli G, Garmestani H, Adams BL. (2004): Microstructure design of a two phase composite using two-point correlation functions. *Journal of Computer-Aided Materials Design* 11 103.

Sankaran S, Zabaras N. (2006): A maximum entropy approach for property prediction of random microstructures. *Acta Materialia* 54:2265.

Schafrik R. (2003): *Technology Transition in Aerospace Industry Workshop on Accelerating Technology Transfer*. National Research Council, Washington DC.

Seidman DN. (2007): Three-Dimensional Atom-Probe Tomography: Advances and Applications. *Annual Review of Materials Research* 37:127.

Shen C, Wang Y. (2003): Phase field model of dislocation networks. *Acta Materialia* 51:2595.

Sivel VGM, Van Den Brand J, Wang WR, Mohdadi H, Tichelaar FD, Alkemade PFA, Zandbergen HW. (2004): Application of the dual-beam FIB/SEM to metals research. *Journal of Microscopy* 214:237.

Tewari A, Gokhale AM, Spowart JE, Miracle DB. (2004): Quantitative characterization of spatial clustering in three-dimensional microstructures using two-point correlation functions. *Acta Materialia* 52:307.

Tong H. (1995): *Non-linear time series: a dynamical system approach*. Oxford; New York: Clarendon Press; Oxford University Press.

Torquato S. (1997): Effective stiffness tensor of composite media–I. Exact series expansions. *Journal of the Mechanics and Physics of Solids* 45:1421.

Torquato S. (2002): *Random Heterogeneous Materials*. New York: Springer-Verlag.

Van Houtte P. (1994): Application of plastic potentials to strain rate sensitive and insensitive anisotropic materials. *International Journal of Plasticity* 10:719.

Wheeler AA, Boettinger WJ, McFadden GB. (1992): Phase-field model for isothermal phase transitions in binary alloys. *Physical Review A* 45:7424.

Yamakov V, Wolf D, Phillpot SR, Mukherjee AK, Gleiter H. (2004): Deformation-mechanism map for nanocrystalline metals by molecular-dynamics simulation. *Nat Mater* 3:43.

Zbib HM, Rhee M, Hirth JP. (1998): On plastic deformation and the dynamics of 3D dislocations. *International Journal of Mechanical Sciences* 40:113.

Zeman J, Ejnoha M. (2007): From random microstructures to representative volume elements. *Modelling and Simulation in Materials Science and Engineering* 15:S325.

Zienkiewicz OC, Taylor RL. (2005): *The Finite Element Method: for solid and structural mechanics*. Oxford [u.a.]: Butterworth-Heinemann.